INTERACTION BETWEEN GAS DIFFUSION AND MULTISTABLE HETEROGENEOUS CHEMICAL KINETICS IN C/C COMPOSITE PROCESSING

Gérard L. VIGNOLES
Université Bordeaux 1, Laboratoire des Composites ThermoStructuraux
3 Allée La Boëtie, F33600 Pessac, France
E-mail: vinhola@lcts.u-bordeaux1.fr

Olivier BACONNEAU and Claude-Michel BRAUNER
Université Bordeaux 1, Mathématiques Appliquées de Bordeaux
351 Cours de la Libération, F33405 Talence cedex, France
E-mail:{Olivier.Baconneau,
Claude-Michel.Brauner}@math.u-bordeaux1.fr

Abstract

The sharpness of the smooth laminar/rough laminar (SL/RL) CVD/CVI pyrocarbon nanotexture transition is addressed in terms of a possible hysteretical chemical deposition mechanism, based on a bimolecular heterogeneous deposition reaction step. Interaction of the hysteretical heterogeneous chemistry with the diffusive transport of the source species enhances the parameter domain of hysteresis, and even better at high Thiele modulus values. A "toy-model" is also studied to explain such a behavior.

Key Words and Phrases. Heterogeneous chemistry, dynamical system, hysteresis, free boundary.

1 Introduction

Aimed at high-temperature, high-performance structural applications, thermostructural composites are made of ceramic or carbon fibers, an interphase which coats them (usually carbon or hexagonal boron nitride), and a matrix which is again either ceramic or carbon. Rocket propeller pieces, aircraft and F-1 racing car brakes are frequently made of carbon/carbon (C/C) composites. To deposit the composite interphase and matrix, a process commonly used is the Isothermal-isobaric Chemical Vapor Infiltration (I-CVI)[1, 2], involving low pressure cracking of gaseous species (precursors), which are

transported mainly by diffusion inside a fibrous preform, where heterogeneous reaction yields a solid deposit which densifies the preform [3]. The gaseous species used for pyrocarbon deposition are hydrocarbons.

Hydrocarbon pyrolysis is well known to lead to various nanotextural forms of pyrocarbon (pyC) in the context of Chemical Vapor Deposition(CVD) and/or Infiltration (CVI) [5, 4]. Among them, two varieties, referred to as Rough Laminar (RL) and Smooth Laminar (SL) because of their appearances when imaged by Optical Microscopy with Polarized Light, differ by their degree of structural anisotropy, and have distinct mechanical and optical properties. A key issue in pyrocarbon CVD/CVI is the control of pyrocarbon nanostructure during processing. It has been shown that the processing parameters are important for this, since SL deposition would be related to small precursor molecules and RL deposition to larger molecules, obtained at later stages of gas-phase hydrocarbon pyrolysis (the so-called *gas phase maturation*) [7, 8, 11, 10, 9]. Additionally, some interesting dynamical behaviors have been discovered for such chemical systems. In the case of pyrocarbon deposition, the transition between SL and RL is "sharp and well defined, without any noticeable transition zone" [8], as confirmed by a more recent study [12]. In the case of silicon carbide deposition from CH_3SiCl_3/H_2 on a plane substrate (*i.e.* CVD), chemical hysteresis between SiC and pyrocarbon deposition regimes has been evidenced as a function of either temperature or added chlorine amount [13]. An explanation for such a fact has been given in terms of a nonlinear Langmuir-Hinshelwood heterogeneous chemical mechanism. The effect of transport was not included in this model, since it is of lesser importance in CVD.

The aim of the present work is to extend to pyrocarbon deposition the modeling approach used for SiC/C codeposition, and in addition to study the effect of gas-phase transport in combination with multistable heterogeneous chemistry. Indeed, as soon as two intermediate species are considered for the deposition of two different pyrocarbons, it is greatly possible that both interact between themselves at the surface, leading naturally to a non-linear cross-reaction term, as is the case for SiC deposition.

The mathematical originality of this problem lies in the fact that it is not the transported species which undergo the multistable chemistry, but another intermediate.

In this work, we set up and analyze simplified model equations collecting the phenomena of interest, in order to better understand the behavior of such a complex physico-chemical system in the context of chemical vapor

infiltration, and also to understand how the hysteretical behavior is modified in the presence of source species diffusion.

2 Model set-up

2.1 Chemical mechanisms

The gas-phase maturation may be translated in a very simplified fashion through a series of homogenenous reactions. The first is the transformation of the initial species R into the first intermediate of interest A, and the second is the transformation of A into another intermediate species B. A and B are respectively precursors of SL and RL pyrocarbons [10, 6].

In our present study, mainly devoted to the reactions occurring close to the substrate, *i.e.* inside the porous medium, we consider for simplicity that the first reaction is already complete, and that the second reaction is similar to a polymerization reaction. So we choose a kinetic model of the form : $nA \rightarrow B$ where n is a small integer.

The precise heterogeneous chemical mechanisms are not well known. We choose a classical Langmuir kinetic scheme (reversible adsorption of the precursor on a surface active site E, followed by an irreversible transformation of the former into the product and a new adsorption site). The fact that the adsorption of B needs n sites is owed to the idea that B is n times larger than A and both A and B are flat (possibly aromatic) molecules.

The whole chemical reaction scheme is summarized below :

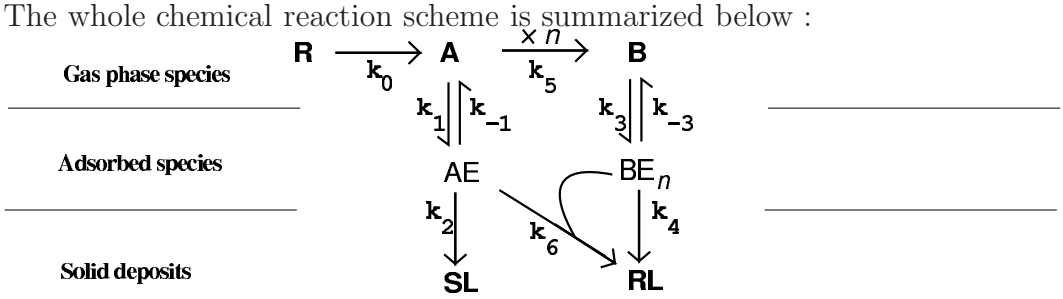

The resulting set of equations arising from this chemical scheme is

$$\left\{\begin{array}{lcl} \mathcal{L}\left([R]\right) & = & -k_0[R], \\ \mathcal{L}\left([A]\right) & = & k_0[R] - k_1[A][E] + k_{-1}[AE] - nk_5[A]^n, \\ \mathcal{L}\left([B]\right) & = & k_5[A]^n - k_3[B][E]^n + k_{-3}[BE_n], \\ \mathcal{L}\left([AE]\right) & = & k_1[A][E] - \left(k_{-1}+k_2\right)[AE] - k_6[AE][BE_n], \\ \mathcal{L}\left([BE_n]\right) & = & k_3[B][E]^n - \left(k_{-3}+k_4\right)[BE_n] - k_6[AE][BE_n], \\ [E]_0 & = & [E] + [AE] + 3[BE_3], \end{array}\right. \tag{2.1}$$

where : (i) the $\mathcal{L}(\bullet)$ operators denote transport and accumulation operators; (ii) the braced symbols denote concentrations ; (iii) $[E]_0$ is the total quantity of adsorption sites per unit surface times the internal surface area; (iv) the constants concerning heterogeneous reactions are implicitly homogenized by taking the internal surface area σ_v (m^{-1}) into account : $k(\text{eff}) = \sigma_v k(\text{het})$.

2.2 General equations

Two kinds of transport of the gaseous species may be considered : convection and diffusion. In the case of isobaric CVI, and taking only account of the porous medium, convection may be safely neglected; diffusion of adsorbed species is considered as a very slow phenomenon with respect to the others ; accordingly, we will approximate $\mathcal{L}(\bullet)$ by $\partial_t \bullet - D_i \partial_{xx} \bullet$ (in 1D geometry) for gaseous species, and $\partial_t \bullet$ for adsorbed species. Moreover, we will restrict ourselves to the case where the precursor species is already completely converted into species A at the entrance of the pores, so that $[R] = 0$ everywhere in the domain of study.

The value of n, the polymerization coefficient, will be set to 3 for the rest of the study, so that the reaction could be 3 $C_2H_2 \longrightarrow C_6H_6$. Under such conditions, the following equations arise from our hypothesis :

$$\left\{\begin{array}{l} \partial_t[A] - D_A\partial_{xx}[A] = -k_1.[A][E] + k_{-1}[AE] - 3k_5[A]^3, \\ \partial_t[B] - D_B\partial_{xx}[B] = -k_3[B][E]^3 + k_{-3}[BE_3] + k_5[A]^3, \\ \partial_t[AE] = k_1[A][E] - k_{-1}[AE] - k_2[AE] - k_6[AE][BE_3], \\ \partial_t[BE_3] = k_3[B][E]^3 - k_{-3}[BE_3] - k_4[BE_3] - k_6[AE][BE_3], \\ [E]_0 = [E] + [AE] + 3[BE_3], \end{array}\right. \tag{2.2}$$

where D_A and D_B are the respective diffusivities of A and B, considered as constants. We have moreover boundary conditions for A and B, Dirichlet

type at $x = 0$, Neumann type at $x = L/2$. As a matter of fact, one should take into account that the porous medium gets progressively plugged by the deposit, usually in a spatially non-homogeneous way [14]. The assumptions that we have made on the diffusion and reaction constants are thus over-simplifications and are only adapted to the study of the initial stage of the process, where the deposit thickness is still very small.

2.3 Dimensionless equations

We define the dimensionless unknowns by

$$a = [A]/[A]_{ref},\ b = [B]/[A]_{ref},\ e = [E]/[E]_0,\ c_1 = [AE]/[E]_0,\ c_2 = [BE_3]/[E]_0\ ,$$

where $[A]_{ref}$ is a reference concentration. Via the scalings $x' = x/L$, $t' = tD_A/L^2$, we get the following dimensionless evolution system (the primes for x and t being omitted) :

$$\left\{\begin{array}{l} \partial_t a - \partial_{xx} a = -\mu_1\, ae + \mu_{-1}\, c_1 - 3\beta a^3, \\ \partial_t b - (D_B/D_A)\, \partial_{xx} b = -\mu_3\, be^3 + \mu_{-3}\, c_2 + \beta a^3, \\ \varepsilon_1\, \partial_t c_1 = \alpha_a\, ae - c_1 - \mu_2\, c_1 c_2, \\ \varepsilon_2\, \partial_t c_2 = \alpha_b\, be^3 - c_2 - \mu_4\, c_1 c_2, \\ c_1 + 3c_2 + e = 1, \\ a(0) = a_0 = 1,\ b(0) = b_0,\ a'(\frac{1}{2}) = \ b'(\frac{1}{2}) = 0 \end{array}\right. \tag{2.3}$$

where :

$$\mu_1 = \frac{k_1 L^2 [E]_0}{D_A},\ \mu_{-1} = \frac{k_{-1} L^2 [E]_0}{D_A [A]_{ref}},\ \beta = \frac{k_5 L^2 [A]_{ref}^2}{D_A}, \mu_3 = \frac{k_3 L^2 [E]_0^3}{D_A},\ \mu_{-3} = \frac{k_{-3} L^2 [E]_0}{D_A [A]_{ref}},$$

$$\alpha_a = \frac{k_1 [A]_{ref}}{k_{-1} + k_2}, \alpha_b = \frac{k_3 [A]_{ref} [E]_0^2}{k_{-3} + k_4},\ \mu_2 = \frac{k_6 [E]_0}{k_{-1} + k_2}, \mu_4 = \frac{k_6 [E]_0}{k_{-3} + k_4},$$

$$\varepsilon_1 = \frac{D_A}{L^2 (k_{-1} + k_2)},\ \varepsilon_2 = \frac{D_A}{L^2 (k_{-3} + k_4)}.$$

The parameter set is provided at Table 1.

3 Hysteretical behavior of the heterogeneous chemical submechanism

Assuming a quasi-steady state, or, in a more mathematical analysis, taking the asymptotic limits as $\varepsilon_1, \varepsilon_2$ go to 0, the last 3 equations of (2.3) define an

Coefficient	Value	Unit	Coefficient	Value	Unit
Heterogeneous chemistry			Gas-phase transport and chemistry		
k_1	10.0	$mol^{-1}.m^3.s^{-1}$	k_5	0.0	$mol^{-2}.m^6.s^{-1}$
k_{-1}	$5.0 \quad 10^{-2}$	s^{-1}	$[A]_{ref}$	0.16	$mol.m^{-3}$
k_2	$3.86 \quad 10^{-2}$	s^{-1}	D_A	10^{-3}	$m^2.s^{-1}$
k_3	509.36	$mol^{-3}.m^9.s^{-1}$	D_B	$5.77 \quad 10^{-4}$	$m^2.s^{-1}$
k_{-3}	0.2	s^{-1}	l	0.05	m
k_4	$6.57 \quad 10^{-2}$	s^{-1}			
k_6	7.0	$mol^{-1}.m^3.s^{-1}$			
$[E]_0$	0.443	$mol.m^{-3}$			

Table 1: Parameter set for the study.

(algebraic) subsystem for (e, c_1, c_2), a and b being given :

$$\begin{cases} 0 = \alpha_a\, ae - c_1 - \mu_2\, c_1 c_2, \\ 0 = \alpha_b\, be^3 - c_2 - \mu_4\, c_1 c_2, \\ c_1 + 3c_2 + e = 1. \end{cases} \tag{3.1}$$

Rearranging Subsystem (3.1), we are led to the computation of the real roots of a polynomial of degree 6 in the unknown $c_2 \in [0, \frac{1}{3}]$ for a given pair (a, b). Then c_1 and e are easily computed. Therefore (3.1) can be described by an equation of the form :

$$G\,(c_2, (a, b)) = 0. \tag{3.2}$$

Standard numerical computations show that, for suitable values of k_6, (3.2) has 3 branches of solutions, see Figure 1a) where we plot c_2 *vs.* b, a being fixed (this parameter is a measure of the degree of gas-phase maturation). Moreover, it is not difficult to compute the eigenvalues of the associated linearized problem and see that the intermediate branch is unstable. The existence of a branch of solutions consisting of unstable equilibria, connecting two stable branches, gives rise to a relay-type hysteresis relationship, say :

$$c_2 = \mathcal{W}[(a, b)], \quad \text{or} \quad (e, c_1, c_2) = \mathcal{W}[(a, b)], \tag{3.3}$$

(a, b) being the *input* and c_2 – or equivalently the triplet (e, c_1, c_2) – the *output*. $\mathcal{W}$ is often called a hysteresis operator [15]. This situation is related to the non-convexity of the underlying potential F with $G = \nabla_{c_2} F$. Each

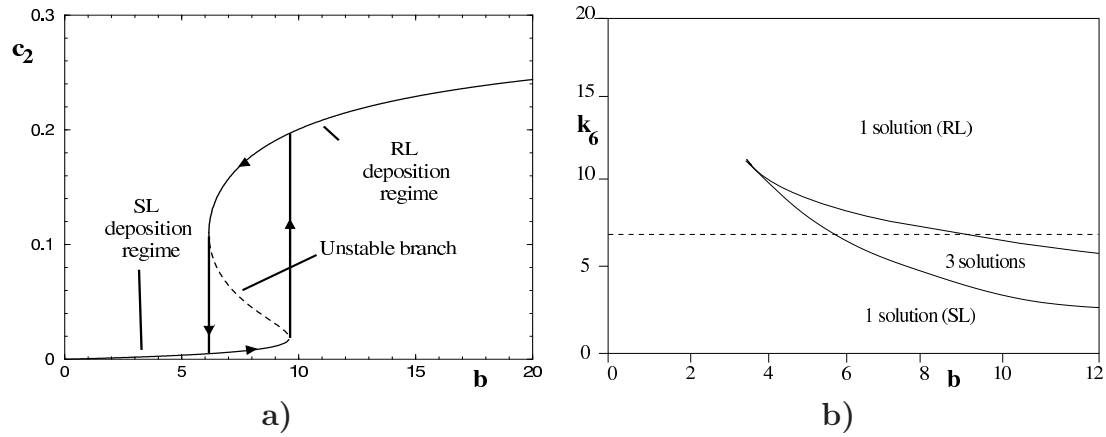

Figure 1: **a)** Diagram of the solution c_2 *vs.* b in subsystem 3.1. **b)** Two-parameter bifurcation diagram of the subsystem representing heterogeneous chemistry. Parameter b represents the extent of gas-phase maturation, while parameter k_6 represents the importance of the bimolecular heterogeneous step.

minimum of the potential corresponds to one kinetic regime of the chemical deposition rate, with a corresponding deposit nanotexture : we may also call them "kinetic phases" by analogy with phase transitions, which are well known as driving mechanisms for hysteresis [16].

It has been conjectured, from a chemical point of view, that this hysteretical behavior is owed to the presence of the cross-reaction term. In order to confirm this guess, we have represented the plan (b, k_6) : actually, Figure 1b) shows that the domain where multiple solutions occur does not intersect $k_6 = 0$, which tends to confirm this conjecture.

4 Numerical results for the full system

System (2.3) can now be replaced by :

$$\left\{\begin{array}{l} \partial_t a - \partial_{xx} a = -\mu_1\, ae + \mu_{-1}\, c_1 - 3\beta a^3, \\ \partial_t b - (D_B/D_A)\, \partial_{xx} b = -\mu_3\, be^3 + \mu_{-3}\, c_2 + \beta a^3, \\ (e, c_1, c_2) = \mathcal{W}[(a, b)], \\ c_1 + 3c_2 + e = 1, \\ a(0) = a_0 = 1,\ b(0) = b_0,\ a'(\frac{1}{2}) = \ b'(\frac{1}{2}) = 0, \end{array}\right. \tag{4.1}$$

that we call hereafter the full or complete system. We are interested in the steady solutions of System (4.1), especially in a hysteresis cycle upon

parameter b_0 and its connection to the hysteresis cycle of Subsystem (3.1). The lack of regularity of some steady solutions close to turning points of the subsystem prevents the use of continuation methods; accordingly, we have limited ourselves to the numerical research of stable steady solutions, thanks to a transient, Crank-Nicholson, finite difference solver, using the result at $b_0 - \delta b_0$ as an initial guess for the result at b_0 and waiting until a steady-state is reached. Two oriented branches have been followed, either starting from $b_0 = 0$ or from b_0 large. Figure 2 shows the hysteresis phenomenon for the complete system, as compared to the heterogeneous subsystem, and answers the above addressed question : one sees readily that diffusion has the effect of enlarging the hysteresis domain. If the diffusion coefficient is increased, then we have a less pronounced enlargement. There are parts of the upper and lower branches of the complete system, lying close to the turning points, which display a Free Boundary (FB) in space between two domains : for example, at the lower branch, close to the center, c_2 is high (RL deposit predominates), and close to the border, c_2 is low (SL deposit predominates), as seen on the inserted plot of $c_2(x)$. The same remark holds at the other side of the hysteresis graph, with inverted geometrical dispositions of SL and RL. Finally, it is also to be noted that the gas-phase species concentrations

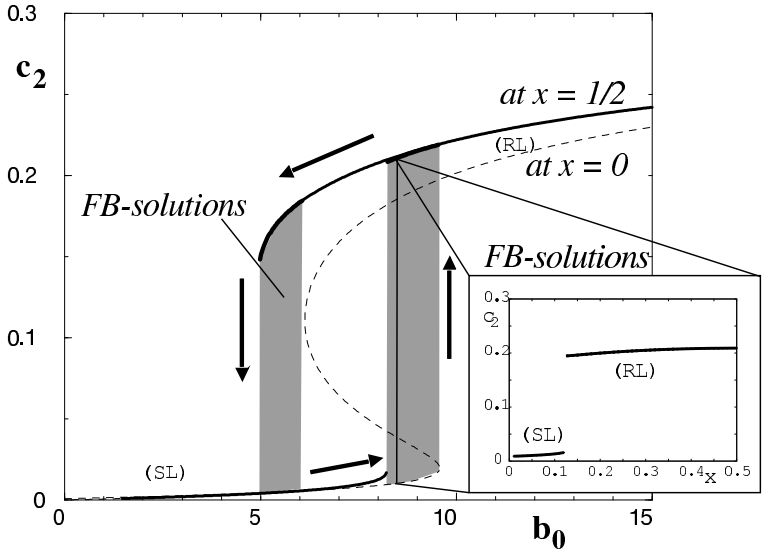

Figure 2: Curves of $c_2(1/2)$ (plain line), and $c_2(0)$ (*i. e.* subsystem (3.1), dotted line) *vs.* b_0 for the full system. Inserted is an example of FB-solution $c_2(x)$.

a and b also undergo a hysteretical behavior, except at $x = 0$.

5 A simple model

For a better understanding of the dynamical behavior of the system, it has been tried to design "the simplest model showing similar behavior" for which solutions would be straightforward to find. For this "toy-model", we choose to represent the heterogeneous subsystem with, as "hysteresis operator", a double Heaviside operator provided with a "path orientation". This operator $\mathcal{H}$ is defined as :

$$\mathcal{H}(u) = \begin{cases} H(d_1 - u) & \text{if } u \text{ is increasing,} \\ H(d_2 - u) & \text{if } u \text{ is decreasing.} \end{cases} \tag{5.1}$$

In (5.1) we take $d_1 > d_2$. However it is worthwhile to begin with the simplest case $d_1 = d_2 = d$. Therefore let $d > 0$ fixed and λ be positive constant. We look for continuously differentiable solutions u :

$$u'' = \lambda^2 u H(d-u),\ x \in (0,1), \quad u'(0) = 0,\ u(1) = b_0, \tag{5.2}$$

where b_0 is a positive parameter. The nonlinear problem (5.2) admits the trivial solutions $u(x) = b_0$ if $b_0 > d$ (case $H(d-u)u \equiv 0$), and $u(x) = b_0 \cosh(\lambda x)/\cosh(\lambda)$ if $b_0 < d$ (case $H(d-u)u = u$). However, there may exist solutions intersecting the line $y = d$, *i.e.* FB-solutions, with Free Boundary $x_0 \in (0,1)$. Problem (5.2) reads :

$$\begin{cases} u''(x) = \lambda^2 u(x) \text{ if } x \in [0, x_0), \quad u''(x) = 0 \text{ if } x \in (x_0, 1), \\ u'(0) = 0, \quad u(1) = b_0, \quad u(x_0) = d, \quad u'(x_0^-) = u'(x_0^+). \end{cases} \tag{5.3}$$

Solving (5.3) is straightforward :

$$u(x) = \frac{b_0 - d}{1 - x_0} x + \frac{d - b_0 x_0}{1 - x_0},\ x \in [x_0, 1], \quad u(x) = \frac{d}{\cosh(\lambda x_0)} \cosh(\lambda x),\ x \in [0, x_0]. \tag{5.4}$$

The regularity of u' at the Free Boundary provides then an equation for the unknown x_0,

$$f_\lambda(x_0) = \lambda(1 - x)\tanh(\lambda x) = \frac{b_0 - d}{d}. \tag{5.5}$$

It is not difficult to prove the following properties :

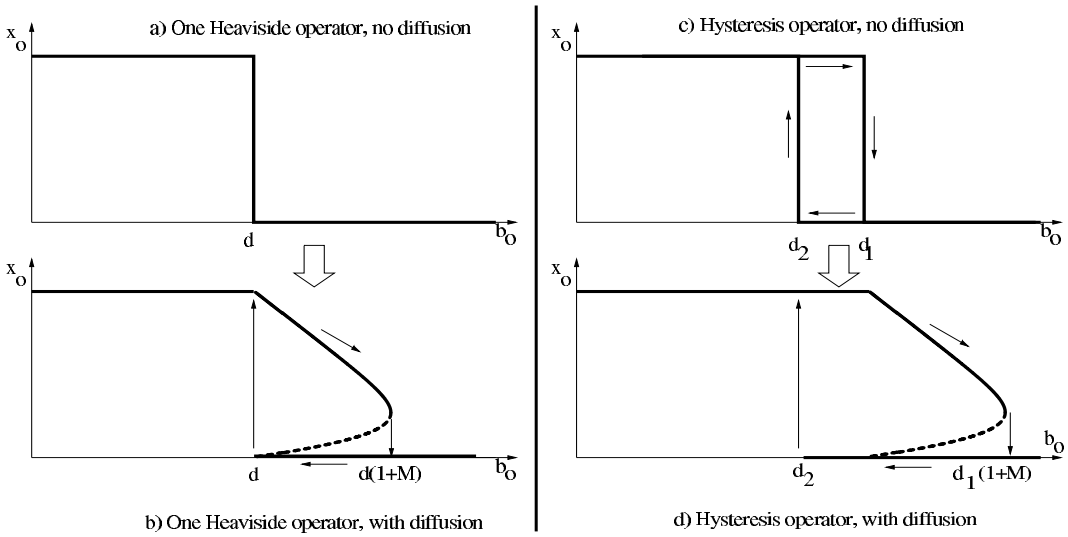

Figure 3: Transformation of the bifurcation diagram by incorporation of diffusion.

- (i) f_λ has a unique maximum $M(\lambda)$ over the interval $[0,1]$, achieved at $x = x_m(\lambda) \in (0, 1/2)$;
- (ii) the function $\lambda \mapsto x_m(\lambda)$ is decreasing, whereas the function $\lambda \mapsto M(\lambda)$ is increasing;
- (iii) for $b_0 = d(1 + M(\lambda))$, there is a unique FB-solution of (5.2);
- (iv) for $d < b_0 < d(1 + M(\lambda))$, problem (5.2) admits 2 FB-solutions;
- (v) for $b_0 < d$ and $d(1+M(\lambda)) < b_0$, problem (5.2) has no FB-solutions.

From a chemical viewpoint, the increase of M with λ , the Thiele modulus, reproduces qualitatively the results for the full system (4.1) with $\beta = 0$. Thus the size of the hysteresis cycle increases when diffusion becomes more and more limiting. We now come back to hysteresis operator (5.1) with $d_1 > d_2$: when b_0 increases, the d_1 branch (upper branch) is used, and the step transition occurs at $b_0 = d_1(1 + M)$ while when b_0 decreases, the d_2 branch (lower branch) is followed. The step transition occurs at $b_0 = d_2$, as sketched at figure 3.

We observe that the result is qualitatively similar to the previous section. It is interesting to note that hysteresis in the reaction-diffusion system is not directly owed to the presence of hysteresis in the heterogeneous subsystem, but rather to the presence of a discontinuity in the source term.

6 Conclusions and perspectives

In order to explain sudden transitions in deposit nanotexture in pyrocarbon CVD/CVI, a dynamical model has been set up, which represents the interaction between gas-phase diffusion and a non-linear heterogeneous chemical mechanism possibly exhibiting hysteresis behavior. It is shown, both numerically and analytically on a simple analogue, that the diffusion of the source species does not destroy the hysteresis behavior, but on the contrary enhances its parameter domain of existence. Indeed, two distinct sources of hysteresis have been evidenced : *i*) the non-linear cross-reaction term arising in the heterogeneous chemistry, and *ii*) the fact that the source term in the diffusion-reaction equation for the gas-phase species is not monotonous. We have verified that these two causes combine together in one broader hysteresis loop. Moreover, close to the turning points, free boundary solutions are found, corresponding to CVI samples containing *e.g.* SL pyrocarbon inside and RL pyrocarbon close to the surface. On the simple analogue, it has been proved that there is only one free boundary point in 1 dimension on the half-domain, in the absence of strong maturation.

The results concerning the simplified model may be extended to somewhat more complicated cases, such as taking maturation into account under the form of a constant negative term in the right-hand side of the b equation of system (5.2). In such a case, the uniqueness of the free boundary point is not any more guaranteed, and "multilayered" solutions could appear. Experimentally, this has been found for the SiC/C codeposition chemical system [17].

References

[1] F. Christin, R. Naslain, C. Bernard, in *Proc. 7th International Conference on CVD*, T. O. Sedgwick and H. Lydtin, Editors, p.499, The Electrochemical Society, Pennington, NJ (1979).

[2] R. Naslain, J.-Y. Rossignol, P. Hagenmuller, F. Christin, L. Héraud, J. J. Choury, *Rev. de Chimie Min.*, **18**, 544 (1981).

[3] J. D. Buckley, in *Proc. 9th Intl. Conf. on Composite Mater. (ICCM-9)* , A. Miravete, Editor, vol. **3**, p. 675, Woodhead Publishing Ltd, New York, and University of Zaragoza (1993).

[4] J. C. Bokros, in *Chemistry and Physics of Carbon* vol. **5**, P. L. Walker Jr., Editor, p. 1, M. Dekker, New York (1969).

[5] P. Loll, P. Delhaès, A. Pacault, A. Pierre, *Carbon*, **15**, 383 (1977).

[6] O. Féron, Ph. D. Thesis, Université Bordeaux 1, n° 1867 (1998).

[7] M. L. Lieberman, H. O. Pierson, *Carbon*, **12**, 233 (1974).

[8] H.O. Pierson, M. L. Lieberman, *Carbon*, **13**, 159 (1975).

[9] P. McAllister, J. F. Hendricks, E. E. Wolf, *Carbon*, **28**, 2505 (1990).

[10] P. Dupel, X. Bourrat, R. Pailler, *Carbon*, **33**, 1193 (1995).

[11] O. Féron, F. Langlais, R. Naslain, J. Thébault, *Carbon*, **37**, 1343 (1999).

[12] J. Lavenac, F. Langlais, O. Féron, R. Naslain, to appear in *Composites Science and Technology* (2001).

[13] G. D. Papasouliotis, S. V. Sotirchos, *J. Electrochem. Soc.*, **145**, 3908 (1998).

[14] S. V. Sotirchos, *AIChE J.* **37**, 1365 (1991).

[15] A. Visintin, *Differential models of hysteresis*, *Appl. Math. Sc.* **111**, Springer Verlag, Heidelberg (1994).

[16] M. Brokate, J. Sprekels, *Hysteresis and phase transition*, *Appl. Math. Sc.* **121**, Springer Verlag, New York (1996).

[17] E. Fitzer, *Chemie-Ing.-Techn.* **41**, 331 (1969).